

# Redox Properties of Cobalt Nitrides for NO Dissociation and Reduction

Zhiwei Yao · Aimin Zhu · C. T. Au ·  
Chuan Shi

Received: 29 November 2008 / Accepted: 27 January 2009 / Published online: 10 February 2009  
© Springer Science+Business Media, LLC 2009

**Abstract** Redox reactions catalyzed by cobalt nitrides should be carried out below the critical temperature at which bulk oxidation of the nitrides occurs. Then, a catalytic redox cycle could be established by introducing a reducing agent into the system below this temperature so that the oxygen could be removed prior to the occurrence of bulk oxidation.

**Keywords** Cobalt nitrides · NO dissociation · Deactivation mechanism · Reducing agent · Catalytic cycle

## 1 Introduction

It is meaningful to explore the catalytic properties of transition metal nitrides because the materials exhibit behaviors similar to those of noble metals. Much of the focus has been on bulk and supported VN, Mo<sub>2</sub>N, W<sub>2</sub>N and Mo/W-based bimetallic (oxy) nitrides due to their competitiveness in NH<sub>3</sub> synthesis [1–3], CO hydrogenation [4],

NO removal [5–12], hydrazine decomposition [13–15], hydrogenation (HYN), hydrodesulfurization (HDS), hydrogenation (HDN) and hydrodeoxygenation (HDO) [16–18] reactions. Being poor in thermal stability, the nitrides of Fe, Co, Re (Group VII–VIII) received far less attention in comparison to their Group V–VI (e.g., V, Mo, W) counterparts [19]. The results of earlier studies indicated that Co<sub>4</sub>N was unstable and underwent stepwise decomposition with N<sub>2</sub> evolution below 700 °C: Co<sub>4</sub>N → Co<sub>3</sub>N + Co, Co<sub>3</sub>N → Co<sub>2</sub>N + Co, Co<sub>2</sub>N → CoN + Co [20]. Kojima and Aika investigated the use of Re<sub>3</sub>N as catalysts for ammonia synthesis (623 K and 0.1 MPa). They reported that despite activity was high initially there was decline in activity in the later stage due to Re<sub>3</sub>N decomposition [21]. To utilize the nitrides of Group VII–VIII transition metals, one has to find a way to improve the thermal stability of these materials. In our recent study [11], Co<sub>4</sub>N particles were dispersed on  $\gamma$ -Al<sub>2</sub>O<sub>3</sub> and the Co<sub>4</sub>N structure could be retained up to a temperature as high as 950 °C. It is envisaged that further studies on interaction between metal nitrides and support materials could result in better thermal stability of Group VII–VIII transition metal nitrides.

Transition metal nitrides have been investigated as potential catalysts for NO removal in the presence or absence of reducing agents. He et al. [5] reported NO conversion of ca. 89% in NO dissociation over Mo<sub>2</sub>N at 450 °C for a period of 10 h. We conducted investigations on NO dissociation and reduction with H<sub>2</sub> over VN, Mo<sub>2</sub>N, W<sub>2</sub>N, and Co<sub>3</sub>Mo<sub>3</sub>N [6–8]. We found that deactivation of VN, Mo<sub>2</sub>N, and W<sub>2</sub>N catalysts was due to various degrees of bulk oxidation, and by increasing the relative concentration of H<sub>2</sub> in NO/H<sub>2</sub>, the lifetime of the catalysts could be extended. In the case of Co<sub>3</sub>Mo<sub>3</sub>N [8], we found that the material was resistant to oxidation during NO/H<sub>2</sub> reaction,

---

Z. Yao · A. Zhu · C. Shi (✉)  
Laboratory of Plasma Physical Chemistry,  
Dalian University of Technology, 116024 Dalian, China  
e-mail: chuanshi@dlut.edu.cn

Z. Yao  
e-mail: mezhiwei@163.com

C. T. Au  
Department of Chemistry, Hong Kong Baptist University,  
Kowloon Tong, Hong Kong, China

C. Shi  
State Key Laboratory of Fine Chemicals,  
Dalian University of Technology, 116024 Dalian, China

exhibiting activity and stability much higher than that of  $\text{Mo}_2\text{N}$ . The phenomenon was explained based on structural consideration. The dissociation and CO reduction of NO over  $\text{Ni}_3\text{N}$  has been reported by Egashira and Komiyama [10]. They found that activity for NO dissociation was high in the initial stage but there was fast deactivation of  $\text{Ni}_3\text{N}$  due to oxidation. When CO was added to aid the removal of surface oxygen species, there was decline in deactivation rate. From these studies, one can come to three important points. First, it is essential to have transition metal nitrides of high thermal stability for catalytic removal of NO. Second, deactivation is due to gradual incorporation of oxygen into the nitride lattice. Third, bulk oxidation and deactivation of nitride catalysts can be mitigated when a reducing agent such as CO or  $\text{H}_2$  is introduced to the feed gas, and as a result the lifetime of catalyst can be prolonged.

In this paper, alumina-supported and unsupported cobalt nitrides were compared for NO dissociation, and two kinds of oxygen-induced deactivation of cobalt nitride were identified. The redox properties of the supported catalyst in NO dissociation and reduction were investigated and a possible route for keeping the catalyst stable and active was proposed.

## 2 Experimental

### 2.1 Sample Preparation

The  $\text{Co}_3\text{O}_4/\gamma\text{-Al}_2\text{O}_3$  precursor with 30wt% Co loading was prepared by stirring  $\gamma\text{-Al}_2\text{O}_3$  ( $S_{\text{BET}} \approx 250 \text{ m}^2 \text{ g}^{-1}$ , 40–60 mesh) in an aqueous cobalt nitrate ( $\text{Co}(\text{NO}_3)_2 \cdot 6\text{H}_2\text{O}$ ) solution, followed by drying at 120 °C for 12 h and calcination at 500 °C for 3 h. The bulk cobalt nitride and  $\gamma\text{-Al}_2\text{O}_3$ -supported cobalt nitride samples were generated by means of  $\text{NH}_3$ -temperature-programmed reaction. Typically, about 2.0 g of the oxide precursor was placed in a micro-reactor and a flow of  $\text{NH}_3$  (150 mL/min) was introduced into the system. Initially, the sample was linearly heated from room temperature (RT) to 300 °C over a period of 30 min followed by a rise in temperature from 300 to 450 °C at a rate of 0.67 °C/min, and a further increase from 450 to 700 °C at a rate of 1.67 °C/min. The temperature was then kept at 700 °C for 2 h before cooling to RT in a  $\text{NH}_3$  flow. The material was then purged with  $\text{N}_2$  for 10 min followed by passivation in 1%  $\text{O}_2/99\% \text{ N}_2$  for 12 h.

The samples of cobalt metal and  $\gamma\text{-Al}_2\text{O}_3$ -supported cobalt metal were prepared from their corresponding oxide precursors under  $\text{H}_2$  at 700 °C for 2 h. The as-obtained materials were then passivated in 1%  $\text{O}_2/99\% \text{ N}_2$  for 12 h before exposure to air.

### 2.2 Sample Characterization

X-ray diffraction (XRD) examination was carried out on an X-ray diffractometer (Rigaku D-Max Rotaflex) with Cu K $\alpha$  radiation and Ni filter. Scanning electron microscopy (SEM) image was obtained using a KYKY 1000 B scanning electron microscope. The sample was covered by a thin film of gold for better image definition. Transmission electron microscopy (TEM) was acquired using a TECNAI G220 transmission electron microscope.

The  $\text{O}_2$  uptake experiments were performed by injecting a standard volume (101  $\mu\text{L}$ ) of pure  $\text{O}_2$  via a calibrated loop at 5 min intervals into the sample using He as carrier gas until there was no detectable uptake of oxygen. Prior to adsorption, the sample was pretreated in He at 400 °C for 1 h. The NO uptake experiments were performed using the same apparatus. The sample (0.05 g) was first treated in He at 400 °C for 1 h and then cooled in He to RT. We kept pulsing NO onto the sample until there was no change in NO signal intensity. The volume of each pulse of NO was 101  $\mu\text{L}$ .

### 2.3 NO Dissociation in the Presence/Absence of Reducing Agent

The NO dissociation reaction was evaluated using a quartz microreactor (i.d. 4 mm). The temperature was measured with a thermocouple placed adjacent to the sample outside the reactor. A reaction gas mixture composed of 1,000 ppm NO, 0 or 1,000 ppm  $\text{H}_2$  and 0 or 1,000 ppm CO in He (balance gas) was fed through the sample (0.4 g, pretreated in pure He at 400 °C for 1 h). At a flow rate of 20 mL/min, the corresponding W/F was 1.2  $\text{g s mL}^{-1}$ . The effluent gasses were monitored by online GC using a molecular sieve 5A column (for the analysis of  $\text{H}_2$ ,  $\text{O}_2$ ,  $\text{N}_2$ , CO and NO) as well as a mass spectrometer (MS, HP G1800A) and an infrared absorption spectrometer (IRAS, SICK-MAI-HAK-S710) (for that of  $\text{NH}_3$ ,  $\text{CO}_2$ ,  $\text{N}_2\text{O}$  and other possible nitrogen oxides).

### 2.4 Catalyst Regeneration

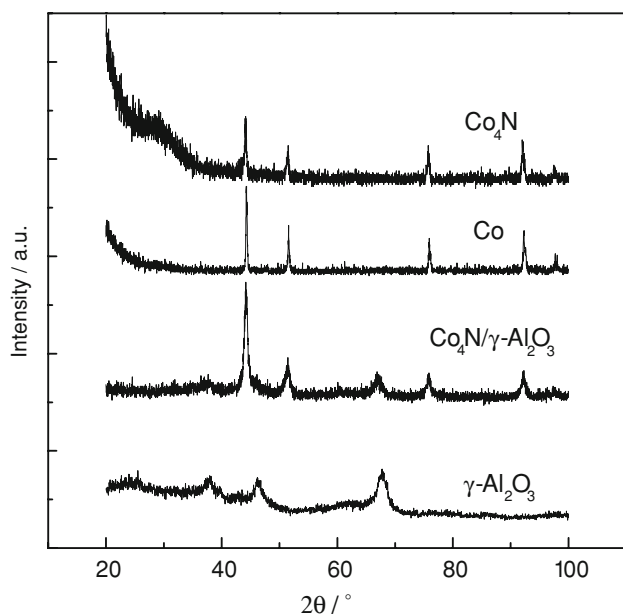
A typical test of successive reaction-regeneration cycles was conducted in a quartz reactor. A reaction gas mixture composed of 1,000 ppm NO and He as balance gas was fed through the sample (0.4 g, pretreated in pure He at 400 °C for 1 h). After deactivation of sample, the flow of 0.1%NO/He was stopped and replaced by a flow of  $\text{H}_2$ . The sample was then treated in  $\text{H}_2$  at 400 °C for 2 h followed by He purging at the same temperature for 1 h. The reaction was again started when a flow of 0.1%NO/He mixture was introduced to the sample at a designated temperature.

### 3 Results

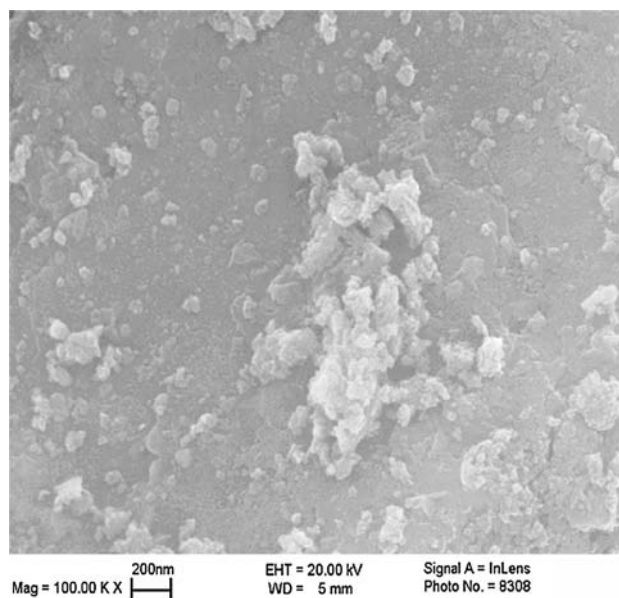
#### 3.1 Structure Characterizations

Figure 1 shows the XRD patterns of  $\text{Co}_4\text{N}$ ,  $\text{Co}_4\text{N}/\gamma\text{-Al}_2\text{O}_3$ , Co metal, and  $\gamma\text{-Al}_2\text{O}_3$ . The XRD patterns of  $\text{Co}_4\text{N}$  and  $\text{Co}_4\text{N}/\gamma\text{-Al}_2\text{O}_3$  are consistent with those reported in the literature for pure  $\text{Co}_4\text{N}$  [22]. Fang et al. [20] reported that the grain structure of  $\text{Co}_4\text{N}$  is similar to that of Co. We also found that it is impossible to differentiate  $\text{Co}_4\text{N}$  from Co because the XRD pattern of  $\text{Co}_3\text{O}_4$  reduced in  $\text{H}_2$  at 700 °C for 2 h looks exactly the same as that of  $\text{Co}_4\text{N}$  (Fig. 1). In our previous papers [11, 12], the results of XPS and temperature-programmed decomposition investigation provide proofs for the formation of bulk  $\text{Co}_4\text{N}$  and  $\text{Co}_4\text{N}/\gamma\text{-Al}_2\text{O}_3$  after the nitridation of their corresponding precursors. According to the XRD data, the crystal size of  $\text{Co}_4\text{N}$  and  $\text{Co}_4\text{N}/\gamma\text{-Al}_2\text{O}_3$  samples estimated by the Scherrer method was 25 and 14, respectively.

The morphology of  $\text{Co}_4\text{N}$  and  $\text{Co}_4\text{N}/\gamma\text{-Al}_2\text{O}_3$  was examined by SEM and TEM technique. The SEM image of  $\text{Co}_4\text{N}$  shows faceted particles composed of agglomerates of irregular shape with size in the range of 20–40 nm (Fig. 2), which matches well with that estimated by the Scherrer method. The aggregation of fine particles is a result of sintering during ammonolysis treatment. Figure 3 presents the low- and high-magnification TEM images of alumina-supported cobalt nitride. As shown in the low-magnification TEM image (Fig. 3a), the  $\text{Co}_4\text{N}$  on the support is oval in shape and is well-dispersed over the support. The corresponding high-magnification TEM image (Fig. 3b)



**Fig. 1** XRD patterns of  $\text{Co}_4\text{N}$ , Co metal,  $\text{Co}_4\text{N}/\gamma\text{-Al}_2\text{O}_3$  and  $\gamma\text{-Al}_2\text{O}_3$



**Fig. 2** SEM image of bulk  $\text{Co}_4\text{N}$

reveals that the oval-shaped  $\text{Co}_4\text{N}$  particles have  $20 \times 25$  nm dimension. The particle size determined by TEM is closed to that estimated by XRD.

#### 3.2 NO and $\text{O}_2$ Uptakes

Figures 4 and 5 show the amount of NO and  $\text{O}_2$  uptakes versus temperature over the  $\text{Co}_4\text{N}$  and  $\text{Co}_4\text{N}/\gamma\text{-Al}_2\text{O}_3$  samples, respectively. From Fig. 4, one can see that below 100 °C, the amount of NO uptake by the two samples was very little. Above 100 °C, the NO uptake increased with temperature; it was  $35 \mu\text{mol g}^{-1}$  at 200 °C and  $95 \mu\text{mol g}^{-1}$  at 400 °C over the  $\text{Co}_4\text{N}/\gamma\text{-Al}_2\text{O}_3$  sample, and  $3 \mu\text{mol g}^{-1}$  at 200 °C and  $29 \mu\text{mol g}^{-1}$  at 400 °C over  $\text{Co}_4\text{N}$ . It indicated that a rise in temperature would enhance the uptake process, and the NO uptake increased quickly over supported  $\text{Co}_4\text{N}$  but slowly over unsupported  $\text{Co}_4\text{N}$ . On the other hand, the amount of oxygen uptake increased with increasing temperature over both samples (Fig. 5). In the case of  $\text{Co}_4\text{N}$  the curve of oxygen uptake drastically increased above 300 °C; it was  $1,470 \mu\text{mol g}^{-1}$  at 400 °C. While in the case of  $\text{Co}_4\text{N}/\gamma\text{-Al}_2\text{O}_3$ , the oxygen uptake increased significantly above 200 °C; it was  $1,276 \mu\text{mol g}^{-1}$  at 300 °C and  $1,622 \mu\text{mol g}^{-1}$  at 400 °C.

#### 3.3 NO Dissociation in the Absence of Reducing Agent

Variation of NO conversion as a function of reaction temperature over  $\text{Co}_4\text{N}$  and  $\text{Co}_4\text{N}/\gamma\text{-Al}_2\text{O}_3$  are shown in Fig. 6. It can be seen that NO dissociation occurred at 200 °C over  $\text{Co}_4\text{N}$ , and the extent of NO dissociation increased with increasing temperature; dissociation of NO

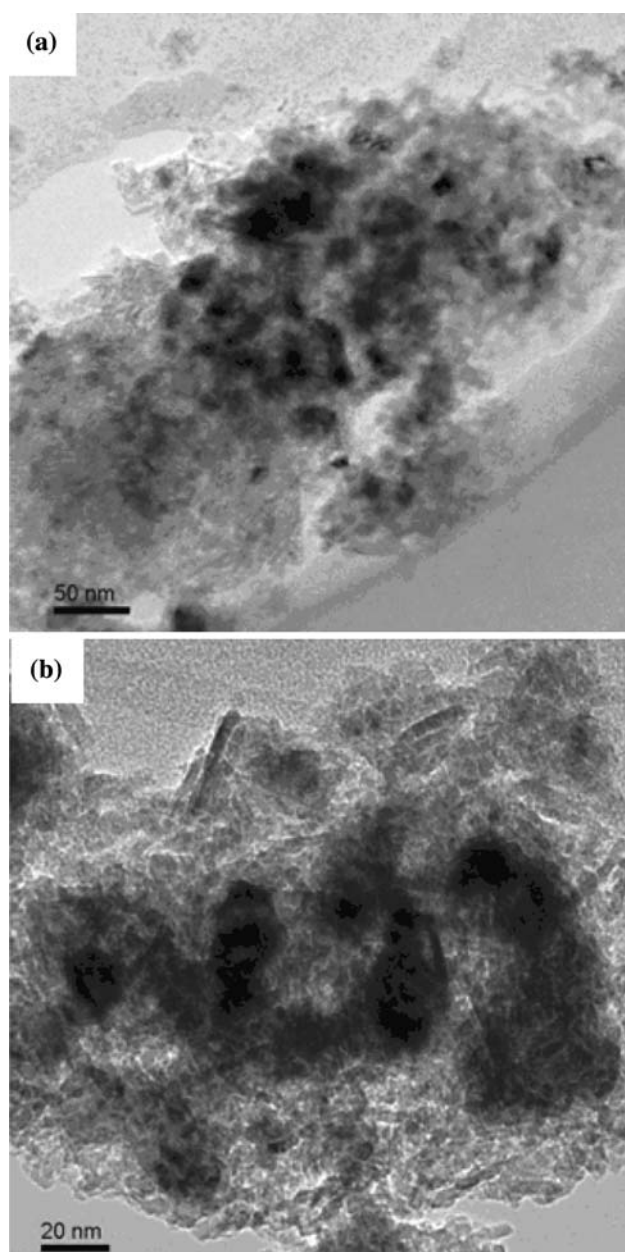


**Fig. 3** **a** Low- and **b** high-magnification TEM images of  $\text{Co}_4\text{N}/\gamma\text{-Al}_2\text{O}_3$

was about half at 250 °C, and complete dissociation NO was detected at 350 °C. Over  $\text{Co}_4\text{N}/\gamma\text{-Al}_2\text{O}_3$ , the degree of NO dissociation was much higher even at lower temperatures: NO dissociation was 60% at 100 °C and 91% at 200 °C. The degree of NO dissociation increased slowly from 200 to 350 °C, and total NO dissociation was achieved at 350 °C. These results indicated that  $\text{Co}_4\text{N}/\gamma\text{-Al}_2\text{O}_3$  showed activity for NO dissociation at lower temperature, and remained active and stable at temperature higher than 450 °C. In the case of  $\text{Co}_4\text{N}$ , decomposition of  $\text{Co}_4\text{N}$  with the evolution of  $\text{N}_2$  occurred above 450 °C (dashed line in Fig. 6). It was worthy to note in Fig. 6 that

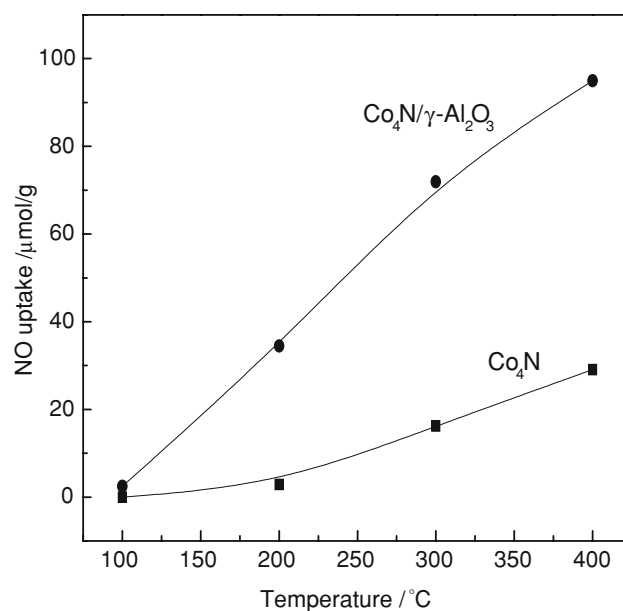


**Fig. 4** NO uptake over  $\text{Co}_4\text{N}$  and  $\text{Co}_4\text{N}/\gamma\text{-Al}_2\text{O}_3$  versus temperature

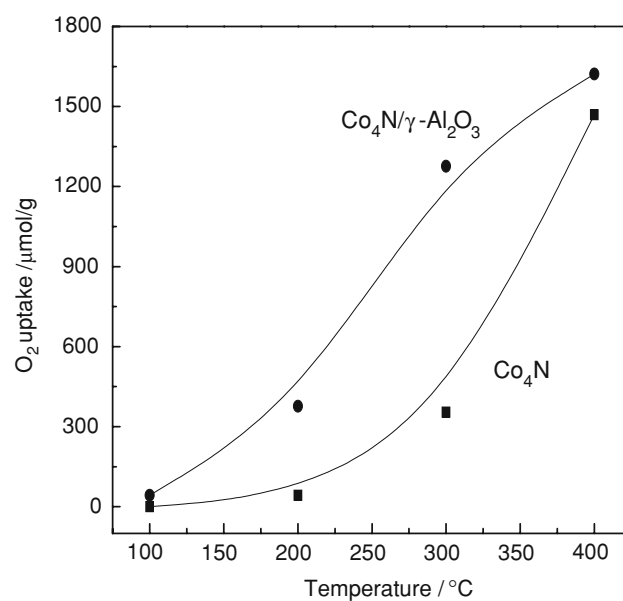


**Fig. 5** Oxygen uptake over  $\text{Co}_4\text{N}$  and  $\text{Co}_4\text{N}/\gamma\text{-Al}_2\text{O}_3$  versus temperature

NO was dissociated to  $\text{N}_2$  over  $\text{Co}_4\text{N}$  and  $\text{Co}_4\text{N}/\gamma\text{-Al}_2\text{O}_3$ , with no detectable production of  $\text{O}_2$ . The results indicated that the oxygen formed by dissociation of NO should chemisorb on  $\text{Co}_4\text{N}$  and  $\text{Co}_4\text{N}/\gamma\text{-Al}_2\text{O}_3$  surfaces or migrate into their bulks at a high temperature. The observations motivated us to investigate the stable activity of NO dissociation on  $\text{Co}_4\text{N}$  and  $\text{Co}_4\text{N}/\gamma\text{-Al}_2\text{O}_3$  catalysts.

Figure 7 shows the time dependence of NO conversion at a given temperature over  $\text{Co}_4\text{N}$  and  $\text{Co}_4\text{N}/\gamma\text{-Al}_2\text{O}_3$ . It can be seen that the durability of unsupported and supported



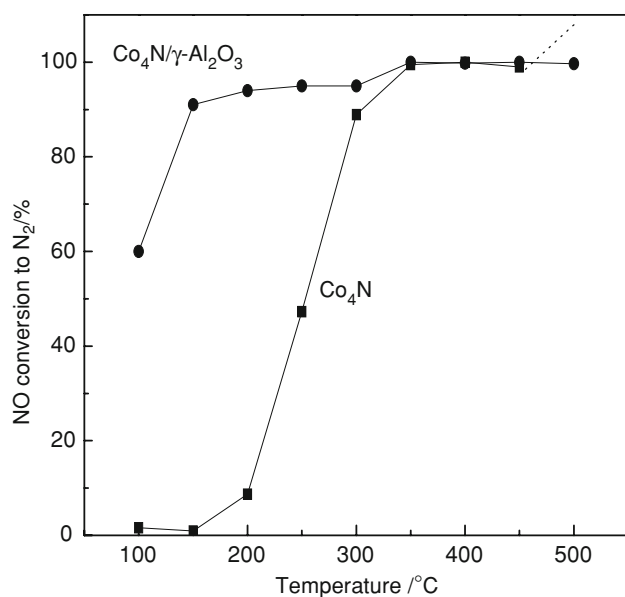
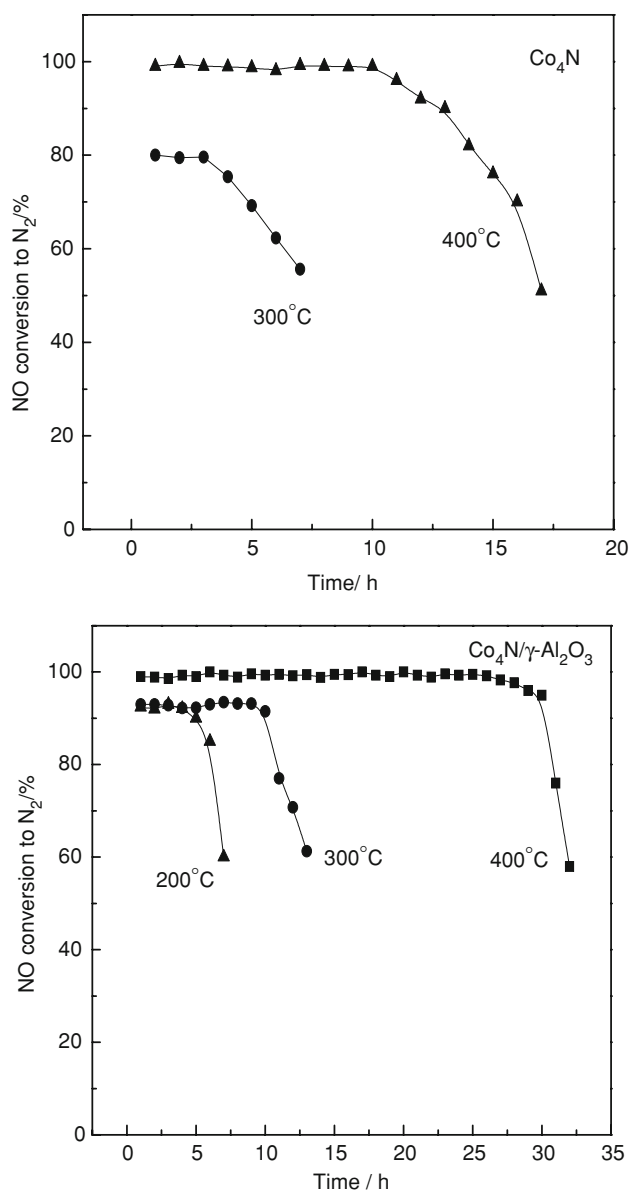


**Fig. 6** Variation of NO conversion as a function of reaction temperature over  $\text{Co}_4\text{N}$  and  $\text{Co}_4\text{N}/\gamma\text{-Al}_2\text{O}_3$ . Reaction conditions:  $\text{NO} = 1,000$  ppm, gas flow rate  $= 20 \text{ cm}^3 \text{ min}^{-1}$ ,  $W/F = 1.2 \text{ gscm}^{-3}$ , reaction time  $= 30$  min

$\text{Co}_4\text{N}$  is strongly dependent on reaction temperature. Over the  $\text{Co}_4\text{N}$  sample, NO conversion (80%) decreased rapidly after 3 h at  $300^\circ\text{C}$  due to deactivation of catalyst. Although the plateau of high activity was prolonged at reaction temperature of  $400^\circ\text{C}$ , deactivation of catalyst occurred after 10 h: NO conversion decreased from ca. 100 to 51% within a period of 17 h. The same is true for  $\text{Co}_4\text{N}/\gamma\text{-Al}_2\text{O}_3$ : a high NO conversion of ca. 90% was attained at  $200^\circ\text{C}$  but there was sharp decrease after 5 h. With temperature increasing to  $300^\circ\text{C}$ , the conversion was ca. 92% and the catalyst started to deactivate after 10 h. As the reaction temperature was further increased to  $400^\circ\text{C}$ , NO conversion of ca. 100% stayed for a long time, and only after 30 h that a drop was detected. It is apparent that despite the lifetime of unsupported and supported cobalt nitrides could be prolonged by increasing the reaction temperature, the effect is temporarily and deactivation of catalysts was inevitable.

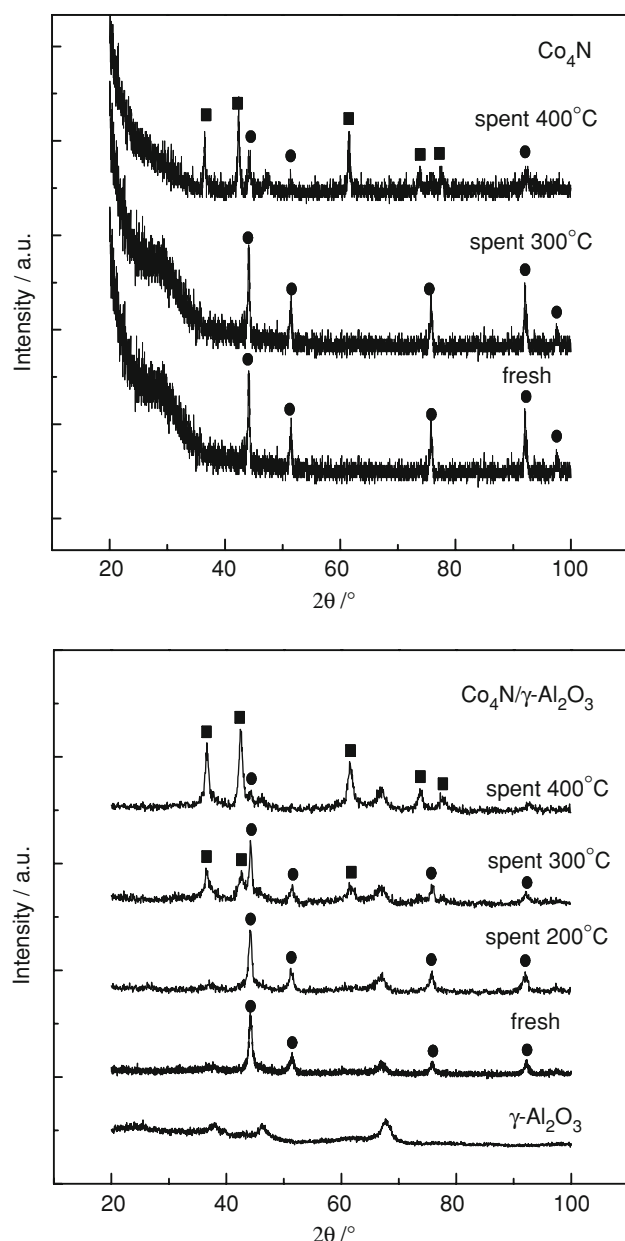
### 3.4 Investigation of Spent Samples

Figure 8 shows the powder XRD patterns of spent samples collected after reaction at various temperatures (see Fig. 7), and for comparison those of fresh catalysts and  $\gamma\text{-Al}_2\text{O}_3$  are also given. Over spent  $\text{Co}_4\text{N}/\gamma\text{-Al}_2\text{O}_3$  sample of  $200^\circ\text{C}$  reaction, the diffraction peaks resemble those of fresh sample, in width as well as in intensity. As for the spent sample of  $300^\circ\text{C}$  reaction, the peaks of CoO (marked ■) coexisted with those of  $\text{Co}_4\text{N}$  (marked ●). The results indicated that certain portion of  $\text{Co}_4\text{N}$  was



**Fig. 7** Time dependence of NO conversion over  $\text{Co}_4\text{N}$  and  $\text{Co}_4\text{N}/\gamma\text{-Al}_2\text{O}_3$  at various reaction temperatures. (Reaction conditions same as those of Fig. 6.)

oxidized to CoO during NO dissociation. The spent  $\text{Co}_4\text{N}/\gamma\text{-Al}_2\text{O}_3$  sample of  $400^\circ\text{C}$  reaction showed peaks of CoO crystallites and the signals of  $\text{Co}_4\text{N}$  was barely traceable. The results indicated that above  $200^\circ\text{C}$  bulk oxidation of  $\text{Co}_4\text{N}$  occurred during NO dissociation over  $\text{Co}_4\text{N}/\gamma\text{-Al}_2\text{O}_3$ , and the degree of  $\text{Co}_4\text{N}$  oxidation increased with increasing temperature, and near complete oxidation of  $\text{Co}_4\text{N}$  occurred at  $400^\circ\text{C}$ . As for the spent  $\text{Co}_4\text{N}$  sample of  $300^\circ\text{C}$  reaction, the diffraction peaks resemble those of fresh  $\text{Co}_4\text{N}$ . It is only after reaction at  $400^\circ\text{C}$  that the spent  $\text{Co}_4\text{N}$  sample indicated the coexistence of CoO and  $\text{Co}_4\text{N}$ , with the signals of the former much more intense than those of the latter. The results indicated that bulk



**Fig. 8** XRD patterns of deactivated samples of various reaction temperatures. The patterns of as-prepared samples and  $\gamma$ - $\text{Al}_2\text{O}_3$  are also shown for comparison. (●)  $\text{Co}_4\text{N}$ , (■)  $\text{CoO}$

oxidation of  $\text{Co}_4\text{N}$  occurred during NO dissociation above 300 °C.

For reactivation, the spent  $\text{Co}_4\text{N}$  and  $\text{Co}_4\text{N}/\gamma\text{-Al}_2\text{O}_3$  samples of low-temperature reaction (300 °C for the bulk  $\text{Co}_4\text{N}$ , 200 °C for supported  $\text{Co}_4\text{N}$ ) were reduced in  $\text{H}_2$  at 400 °C. Figure 9 shows the results of three successive reaction/regeneration cycles. It is clear that NO conversion was almost the same across the three successive runs, verifying that the spent  $\text{Co}_4\text{N}$  and  $\text{Co}_4\text{N}/\gamma\text{-Al}_2\text{O}_3$  catalysts of low-temperature reaction can be reactivated by means of  $\text{H}_2$  treatment.

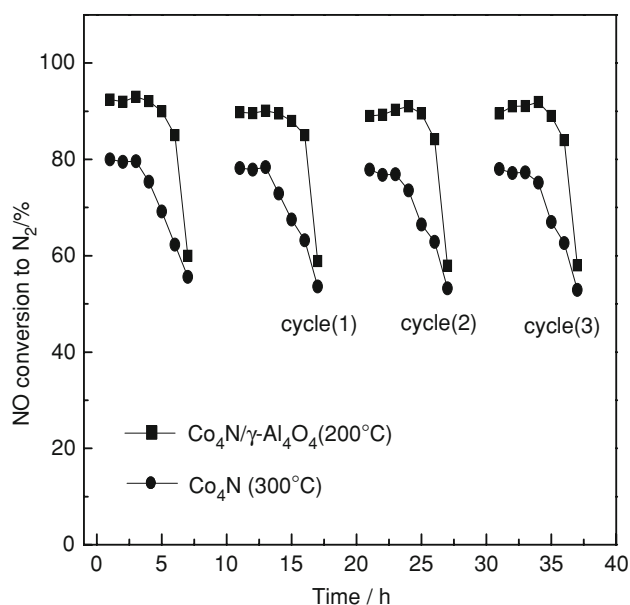


**Fig. 9** Deactivation and regeneration of  $\text{Co}_4\text{N}$  and  $\text{Co}_4\text{N}/\gamma\text{-Al}_2\text{O}_3$  samples in multicycle tests. (Reaction conditions same as those of Fig. 6.) The deactivated  $\text{Co}_4\text{N}$  and  $\text{Co}_4\text{N}/\gamma\text{-Al}_2\text{O}_3$  samples were activated via reduction at 400 °C for 2 h in a flow of pure  $\text{H}_2$

### 3.5 NO Dissociation in the Presence of Reducing Agent

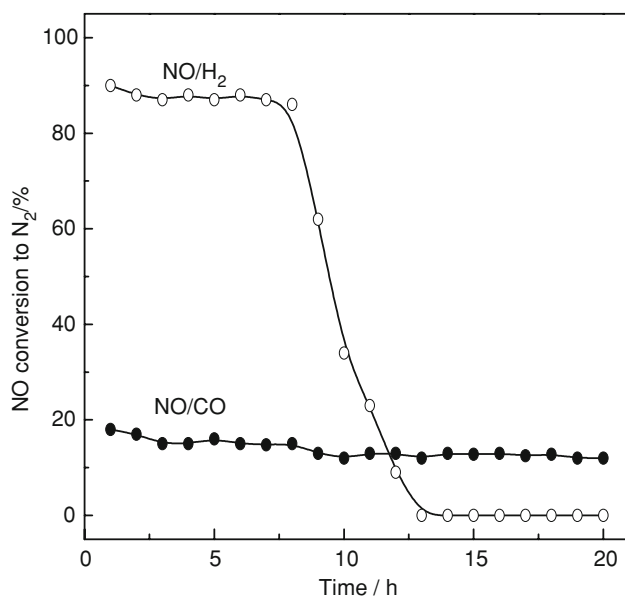
Table 1 shows the catalytic activities of NO dissociation in the presence of  $\text{H}_2$  or CO over  $\text{Co}_4\text{N}/\gamma\text{-Al}_2\text{O}_3$ . When  $\text{H}_2$  was added to the NO feed, the  $\text{Co}_4\text{N}/\gamma\text{-Al}_2\text{O}_3$  catalyst showed high activity for conversion of NO to  $\text{N}_2$  (87%) at 200 °C, and 100% NO conversion to  $\text{N}_2$  was achieved at or above 400 °C. The conversion of  $\text{H}_2$  over  $\text{Co}_4\text{N}/\gamma\text{-Al}_2\text{O}_3$  is an activated process and is temperature dependent. One can see that  $\text{H}_2$  conversion was only 30% at 200 °C and increased to 92% at 600 °C. Above 600 °C, there was a decline in NO reduction plausibly due to the large extent of NO dissociation on  $\text{Co}_4\text{N}/\gamma\text{-Al}_2\text{O}_3$  surface. On the other hand, when CO was introduced as reducing agent, conversion of NO to  $\text{N}_2$  and CO was 15 and 23% at 200 °C, respectively, significantly lower in NO conversion to  $\text{N}_2$  in comparison with that of the NO/ $\text{H}_2$  reaction (i.e., 87%). The catalytic behavior of  $\text{Co}_4\text{N}/\gamma\text{-Al}_2\text{O}_3$  in NO/CO at temperatures above 200 °C shows trends similar to those in NO/ $\text{H}_2$ : NO conversion to  $\text{N}_2$  reached 100% at 400 °C and CO conversion increased with increasing temperature, reaching 82% at 600 °C and declined slightly to 79% at 700 °C. As shown in Table 1, the conversion of reducing agent ( $\text{H}_2$  or CO) was much lower than that of NO at any temperature, except in the case of NO/CO at 200 °C in which the conversion of CO was slightly higher than that of NO. It was worthy to note that the  $\text{Co}_4\text{N}/\gamma\text{-Al}_2\text{O}_3$  showed a activity of 94% NO conversion without  $\text{H}_2$  or CO at 200 °C

**Table 1** Catalytic activities of NO dissociation in the presence of H<sub>2</sub> or CO over Co<sub>4</sub>N/ $\gamma$ -Al<sub>2</sub>O<sub>3</sub>

T/°C	Conversion (%)			
	NO/H <sub>2</sub> system		NO/CO system	
	NO to N <sub>2</sub>	H <sub>2</sub>	NO to N <sub>2</sub>	CO
200	87	30	15	23
300	92	56	86	62
400	100	78	100	74
600	100	92	100	82
700	100	61	100	79

Reaction conditions: NO = 1,000 ppm, H<sub>2</sub> or CO = 1,000 ppm, gas flow rate = 20 cm<sup>3</sup> min<sup>-1</sup>, W/F = 1.2 gscm<sup>-3</sup>, reaction time = 8 h

(Fig. 6), however, the conversion of NO decreased to 87% in the presence of H<sub>2</sub> and 12% in the presence of CO (Table 1). This was because, there was a competition in adsorption between NO and reducing agent (H<sub>2</sub> or CO) on nitride surfaces, as suggested before [6, 7]. Once the surface active sites were not very effective for co-adsorption of NO and reducing agent (H<sub>2</sub> or CO), the amount of adsorbed and dissociated NO would reduce and hence the conversion of NO to N<sub>2</sub> would decrease correspondingly. Figure 10 shows the time dependence of NO conversion over Co<sub>4</sub>N/ $\gamma$ -Al<sub>2</sub>O<sub>3</sub> at 200 °C in NO/CO and NO/H<sub>2</sub> reaction. In NO/H<sub>2</sub> reaction, Co<sub>4</sub>N/ $\gamma$ -Al<sub>2</sub>O<sub>3</sub> showed high initial activity of ca. 87% NO conversion to N<sub>2</sub> but deactivated rapidly after 8 h, showing 0% NO conversion to N<sub>2</sub> at 13 h. In the case of NO/CO, Co<sub>4</sub>N/ $\gamma$ -Al<sub>2</sub>O<sub>3</sub> showed

**Fig. 10** Time dependence of NO conversion over Co<sub>4</sub>N/ $\gamma$ -Al<sub>2</sub>O<sub>3</sub> at 200 °C in NO/H<sub>2</sub> and NO/CO. Reaction conditions: NO = 1,000 ppm, H<sub>2</sub> or CO = 1,000 ppm, gas flow rate = 20 cm<sup>3</sup> min<sup>-1</sup>, W/F = 1.2 gscm<sup>-3</sup>

relatively lower activity (ca. 12%) but was catalytically stable throughout the entire period of 20 h.

## 4 Discussion

The nitrides and carbides of transition metals show catalytic properties similar to those of noble metals [14]. In the formation of nitrides and carbides, there is contraction of metal d band and greater density of states near the Fermi level. The result is catalytic properties different from those of the parent metals but similar to those of noble metals [23, 24]. It is well known that noble metal catalysts are catalytically active in decomposition and reduction of NO<sub>x</sub>, and are used as active components in three-way catalyst (TWC) converters [25, 26]. The similarity in chemical properties between transition metal nitrides and noble metals suggests that the former could be active for NO adsorption and dissociation.

### 4.1 Catalyst Deactivation

Due to small crystal size and big surface area as well as the strong interaction of Co<sub>4</sub>N and  $\gamma$ -Al<sub>2</sub>O<sub>3</sub>, Co<sub>4</sub>N/ $\gamma$ -Al<sub>2</sub>O<sub>3</sub> showed much higher activity for NO dissociation than Co<sub>4</sub>N at 200 °C [11, 12]. While both Co<sub>4</sub>N and Co<sub>4</sub>N/ $\gamma$ -Al<sub>2</sub>O<sub>3</sub> deactivate during NO dissociation, the latter shows better performance than the former. Based on the results of XRD characterization (Fig. 8), it can be deduced that deactivation of Co<sub>4</sub>N during NO dissociation at 400 °C is mainly due to Co<sub>4</sub>N bulk oxidation. The same applies to Co<sub>4</sub>N/ $\gamma$ -Al<sub>2</sub>O<sub>3</sub> during NO dissociation above 300 °C. Nevertheless, the deactivation of catalysts at lower temperatures ( $\leq 300$  °C for Co<sub>4</sub>N,  $\leq 200$  °C for Co<sub>4</sub>N/ $\gamma$ -Al<sub>2</sub>O<sub>3</sub>) might not be due to bulk oxidation as suggested by the results of XRD studies (Fig. 8). The idea is confirmed by the results of H<sub>2</sub>-regeneration experiments where spent Co<sub>4</sub>N and Co<sub>4</sub>N/ $\gamma$ -Al<sub>2</sub>O<sub>3</sub> of low-temperature reactions could be reactivated (Fig. 9).

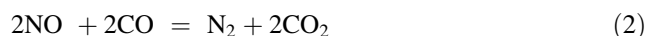
One can gain a better understanding on the interaction of oxygen with the surface of Co<sub>4</sub>N by looking into the results of oxygen uptake experiments (Fig. 5). The results indicated that oxygen uptake on both samples is an activated process. At low temperatures ( $\leq 300$  °C for Co<sub>4</sub>N,  $\leq 200$  °C for Co<sub>4</sub>N/ $\gamma$ -Al<sub>2</sub>O<sub>3</sub>), the oxygen is primarily absorbed on the surface. A rise in temperature would cause a rapid increase in O<sub>2</sub> uptake, probably due to diffusion of surface oxygen into Co<sub>4</sub>N lattice and start of bulk oxidation. In order to confirm whether the steep slope in O<sub>2</sub>-uptake profile was due to progressive oxidation of cobalt nitrides, we heated the as-prepared Co<sub>4</sub>N and Co<sub>4</sub>N/ $\gamma$ -Al<sub>2</sub>O<sub>3</sub> samples at 320 and 220 °C, respectively, in air for 2 h. Subsequent XRD analysis (not shown) of both samples

yielded cobalt oxide phase. This is an important piece of information and since bulk oxidation of  $\text{Co}_4\text{N}$  occurred above 300 °C and that of  $\text{Co}_4\text{N}/\gamma\text{-Al}_2\text{O}_3$  above 200 °C, the structure of the catalysts are intact in low-temperature reactions ( $\leq 300$  °C for  $\text{Co}_4\text{N}$ ,  $\leq 200$  °C for  $\text{Co}_4\text{N}/\gamma\text{-Al}_2\text{O}_3$ ) as confirmed in XRD studies (Fig. 8). We propose that there are two kinds of deactivation mechanism for NO dissociation over  $\text{Co}_4\text{N}$ -based catalysts. First, the surface of  $\text{Co}_4\text{N}$  is covered with chemisorbed oxygen originated from NO dissociation, and NO adsorption and dissociation cease. Nevertheless, the deactivation is temporary and the spent catalyst can be completely reactivated via removal of surface oxygen by means of  $\text{H}_2$ -reduction (Fig. 9). Second, the diffusion of surface oxygen into the bulk of  $\text{Co}_4\text{N}$  during high-temperature reactions ( $> 300$  °C for  $\text{Co}_4\text{N}$ ,  $> 200$  °C for  $\text{Co}_4\text{N}/\gamma\text{-Al}_2\text{O}_3$ ) would result in bulk oxidation and permanent deactivation of catalyst.

Based on the deactivation mechanism mentioned above, it is confirmed that the oxygen generated from NO dissociation is not evolved on  $\text{Co}_4\text{N}$  and  $\text{Co}_4\text{N}/\gamma\text{-Al}_2\text{O}_3$  catalysts at any temperature. It can therefore be said that  $\text{Co}_4\text{N}$  and  $\text{Co}_4\text{N}/\gamma\text{-Al}_2\text{O}_3$  catalysts are catalytic but not effective for the self-dissociation of NO at low temperature ( $\leq 300$  °C for  $\text{Co}_4\text{N}$ ,  $\leq 200$  °C for  $\text{Co}_4\text{N}/\gamma\text{-Al}_2\text{O}_3$ ); NO dissociation reactions proceed non-catalytically at high temperature ( $> 300$  °C for  $\text{Co}_4\text{N}$ ,  $> 200$  °C for  $\text{Co}_4\text{N}/\gamma\text{-Al}_2\text{O}_3$ ), consuming cobalt nitride to yield those of corresponding oxide(s).

## 4.2 Removal of Surface Oxygen

It is hence clear that the adoption of a reducing agent for the removal of surface oxygen is beneficial for maintaining a steady-state of NO dissociation. In the reactions of NO reduction with  $\text{H}_2$  or CO, the following stoichiometric conversions (Eqs. 1 and 2) of NO to  $\text{N}_2$  are expected:



From the data at the temperature above 200 °C in Table 1, the conversion of NO to  $\text{N}_2$  is much higher than that of reducing agent ( $\text{H}_2$  or CO), indicating that the self-dissociation of NO on supported cobalt nitride catalyst occurs to yield a portion of  $\text{N}_2$ , but oxygen generated from NO dissociation was captured by the catalyst. In other words, in NO/ $\text{H}_2$  and NO/CO reactions, oxygen from NO dissociation would inevitably incorporate into the bulk of  $\text{Co}_4\text{N}/\gamma\text{-Al}_2\text{O}_3$  catalyst above 200 °C, and hence can not be removed completely by reducing agent. The results have been verified by  $\text{O}_2$ -uptake and XRD measurements as shown in Figs. 5 and 8. Therefore, in order to obtain a steady-state NO dissociation, the reducing agent has to be

effective below the temperature at which diffusion of surface oxygen into bulk occurs. During NO/ $\text{H}_2$  and NO/CO reactions at 200 °C, the nitrogen-containing reaction products is only  $\text{N}_2$ , without  $\text{N}_2\text{O}$ ,  $\text{NH}_3$  (in the case of  $\text{H}_2$ ) and other nitrogen oxides by analysis of MS and IRAS. The product of  $\text{N}_2$  can be originated from the reactions (Eqs. (1) and (2)) and the self-dissociation of NO on  $\text{Co}_4\text{N}/\gamma\text{-Al}_2\text{O}_3$  catalyst. Thus, we believe that a steady-state NO dissociation can be obtained when a completely stoichiometrical conversion of NO and reducing agent ( $\text{H}_2$  or CO) seems to be achieved. From Table 1, in the case of  $\text{H}_2$  as reducing agent,  $\text{H}_2$  and NO conversion at 200 °C over  $\text{Co}_4\text{N}/\gamma\text{-Al}_2\text{O}_3$  was 30 and 87%, respectively. The results reveal that despite NO dissociation is effective at 200 °C, only a minor part of oxygen was removed by  $\text{H}_2$  (Table 1). In the case of CO as reducing agent, CO and NO conversion at 200 °C was 23 and 15%, respectively. The data indicated that although the extent of NO dissociation was relatively lower in comparison to that of the NO/ $\text{H}_2$  case, the oxygen originated from NO dissociation can be effectively captured and removed by CO. The conversion of NO and CO is non-stoichiometric with the latter higher than the former. Considering the passivation procedure in catalyst preparation, there would be surface oxygen prior to NO adsorption, and the extra oxygen would mean CO conversion larger than NO conversion. It is obvious that a catalytic cycle can be established over  $\text{Co}_4\text{N}/\gamma\text{-Al}_2\text{O}_3$  at 200 °C in NO/CO reaction. As in the case of NO/ $\text{H}_2$ , the oxygen produced in NO dissociation is captured by the catalyst in large proportion. With heavy accumulation of surface oxygen on  $\text{Co}_4\text{N}/\gamma\text{-Al}_2\text{O}_3$ , there is deactivation of catalyst with reaction time (Fig. 10).

## 5 Conclusions

Bulk and  $\gamma\text{-Al}_2\text{O}_3$ -supported  $\text{Co}_4\text{N}$  were synthesized by  $\text{NH}_3$ -temperature-programmed reaction, and their redox properties for NO dissociation and reduction were investigated. We found that the lifetime of  $\text{Co}_4\text{N}$  can be prolonged by increasing the reaction temperature but the catalysts still suffer from deactivation in NO dissociation reaction. As indicated by the results of XRD and catalyst regeneration experiments, there are two kinds of deactivation mechanism. (1) Heavy accumulation of surface oxygen generated in NO dissociation at low temperatures ( $\leq 300$  °C for  $\text{Co}_4\text{N}$ ,  $\leq 200$  °C for  $\text{Co}_4\text{N}/\gamma\text{-Al}_2\text{O}_3$ ) would cause temporary deactivation of catalysts. By reduction with  $\text{H}_2$ , the samples can be reactivated. (2) The diffusion of surface oxygen into the lattice of  $\text{Co}_4\text{N}$  at high temperatures ( $> 300$  °C for  $\text{Co}_4\text{N}$ ,  $> 200$  °C for  $\text{Co}_4\text{N}/\gamma\text{-Al}_2\text{O}_3$ ) would result in bulk oxidation and permanent deactivation of catalysts. Therefore,  $\text{Co}_4\text{N}$  and  $\text{Co}_4\text{N}/\gamma\text{-Al}_2\text{O}_3$  catalysts are catalytic but not effective



for low-temperature NO dissociation; NO dissociation reactions proceed non-catalytically at high temperatures, consuming cobalt nitride to yield those of corresponding oxide(s). Clearly, it is advisable to establish a steady-state of NO dissociation over  $\text{Co}_4\text{N}/\gamma\text{-Al}_2\text{O}_3$  when a suitable reducing agent is adopted for the complete removal of surface oxygen at a temperature low enough to avoid bulk oxidation. We found that surface oxygen from NO dissociation could be effectively removed by CO at 200 °C, and cycles of catalytic dissociation of NO can be achieved using  $\text{Co}_4\text{N}/\gamma\text{-Al}_2\text{O}_3$  as catalyst.

**Acknowledgments** The work was supported by the National Natural Science Foundation of China (No. 20573014) and by the Program for New Century Excellent Talents in University (NCET-07-0136).

## References

1. Kojima R, Aika K-I (2001) *Appl Catal A* 219:141
2. Kojima R, Aika K-I (2001) *Appl Catal A* 219:157
3. Jacobsen CJH (2000) *Chem Commun* 1057
4. Ranhotra GS, Bell AT, Reimer JA (1987) *J Catal* 108:40
5. He H, Dai HX, Ngan KY, Au CT (2001) *Catal Lett* 71:147
6. Shi C, Yang XF, Zhu AM, Au CT (2004) *Catal Today* 93–95:819
7. Shi C, Zhu AM, Yang XF, Au CT (2004) *Appl Catal A* 276:223
8. Shi C, Yang XF, Zhu AM, Au CT (2004) *Catal Lett* 97:9
9. Shi C, Zhu AM, Yang XF, Au CT (2005) *Appl Catal A* 293:83
10. Egashira Y, Komiyama H (1990) *Ind Eng Chem Res* 29:1583
11. Yao ZW, Zhu AM, Chen J, Wang XK, Au CT, Shi C (2007) *J Solid State Chem* 180:2635
12. Yao ZW, Zhang AJ, Li Y, Zhang YZ, Cheng XQ, Shi C (2008) *J Alloys Compd* 464:488
13. Rodrigues JAJ, Cruz GM, Bugli G, Boudart M, DjegaMariadasou G (1997) *Catal Lett* 45:1
14. Chen XW, Zhang T, Zheng MY, Wu ZL, Wu WC, Li C (2004) *J Catal* 224:473
15. Chen XW, Zhang T, Li C, Xia LG, Li T, Zheng MY, Wu ZL, Wang XD, Wei ZB, Xin Q (2002) *Catal Lett* 79:21
16. Furimsky E (2003) *Appl Catal A* 240:1
17. Yu CC, Ramanathan S, Oyama ST (1998) *J Catal* 173:1
18. Ramanathan S, Yu CC, Oyama ST (1998) *J Catal* 173:10
19. Oyama ST (1996) *The chemistry of transition metal carbides and nitrides*. Blackie, New York
20. Fang JS, Yang LC, Hsu CS, Chen GS, Lin YW, Chen GS (2004) *J Vac Sci Technol A* 22:698
21. Kojima R, Aika K (2001) *Appl Catal A* 209:317
22. Milad IK, Smith KJ, Wong PC, Mitchell KAR (1998) *Catal Lett* 52:113
23. Colling CW, Thompson LT (1994) *J Catal* 146:193
24. Nagai M, Miyao T, Tuboi T (1993) *Catal Lett* 18:9
25. Tabata F (1988) *J Mater Sci Lett* 7:147
26. Yang RT, Chen N (1994) *Ind Eng Chem Res* 33:825